Energy Conversion and Management: X 20 (2023) 100438

Contents lists available at ScienceDirect

Energy Conversion and Management: X

journal homepage: www.sciencedirect.com/journal/energy-conversion-and-management-x

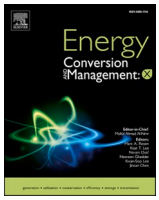

AI-driven optimization of ethanol-powered internal combustion engines in alignment with multiple SDGs: A sustainable energy transition

Muhammad Usman [a], Muhammad Kashif Jamil [a], Waqar Muhammad Ashraf [c,*], Syed Saqib [a], Touqeer Ahmad [a], Yasser Fouad [b], Husnain Raza [a], Umar Ashfaq [a], Aamir Pervaiz [a]

[a] Department of Mechanical Engineering, University of Engineering and Technology, Lahore, Pakistan
[b] Department of Applied Mechanical Engineering, College of Applied Engineering, Muzahimiyah Branch, King Saud University, P.O. Box 800, Riyadh 11421, Saudi Arabia
[c] The Sargent Centre for Process Systems Engineering, Department of Chemical Engineering, University College London, Torrington Place, London WC1E 7JE, United Kingdom

ARTICLE INFO

Keywords:
Artificial neural network
Prediction
Response surface methodology
Optimization
Alcoholic fuel
SDG

ABSTRACT

With the escalating requirement for global sustainable energy solutions and the complexities linked with the complete transition to new technologies, internal combustion engines (ICEs) powered with biofuels like ethanol are gaining significance over time. However, problems linked to the performance and emissions of such ICEs necessitate accurate prediction and optimization. The study employed the integration of artificial neural networks (ANN) and multi-level historical design of response surface methodology (RSM) to address these challenges in alignment with the Sustainable Development Goals (SDGs). A single-cylinder spark ignition (SI) engine powered with ethanol-gasoline blends at different loads and speeds was used to gather data. Among six initially trained ANN models, the most efficient model with a regression coefficient (R^2) of 0.9952 (training), 0.98579 (validation), 0.98847 (testing), and 0.99307 (overall) was employed to predict outputs such as brake power, brake specific fuel consumption (BSFC), brake thermal energy (BTE), concentration of carbon dioxide (CO_2), carbon monoxide (CO), hydrocarbons (HC), and oxides of nitrogen NOx. Predicted outputs were optimized by incorporating RSM. On implementing optimized conditions, it was observed that BP and BTE increased by 19.9%, and 29.8%, respectively. Additionally, CO, and HC emissions experienced substantial reductions of 28.1%, and 40.6%, respectively. This research can help engine producers and researchers make refined decisions and achieve improved performance and emissions. The study directly supports SDG 7, SDG 9, SDG 12, SDG 13, and SGD 17, which call for achieving affordable, clean energy, sustainable industrialization, responsible consumption, and production, taking action on climate change, and partnership to advance the SDGs as a whole respectively.

Introduction

It is estimated that by 2050, there will be 9.2 billion people on the planet, with the transport industry potentially consuming over one-third of the world's energy and more than half of total oil production [1,2]. In line with the issues addressed by the Sustainable Development Goals (SDGs), this population upsurge and industrial expansion have resulted in the unavoidable depletion of conventional fuels and increasing threats to environmental sustainability, energy security, and economic stability. Alternative fuels such as biofuels and hydrogen for internal combustion engines (ICEs) are thought to provide solutions to these problems [3–6]. Investigation of these alternative fuels directly promotes SDGs 7 (Affordable and Clean Energy) and 13 (Climate Action), which reinforce transitioning to sustainable and clean energy sources to address climate change. SGD 7 highlights the significance of switching from polluting and unsustainable energy sources to cleaner ones. Additionally, it assists in establishing a balance between addressing the urgent need to combat climate change, promoting economic growth, and fulfilling energy demands. [7–9]. However, the complete transition to new technologies encounters socio-technological obstacles and

* Corresponding author.
E-mail addresses: muhammadusman@uet.edu.pk (M. Usman), kashif.jamil@uet.edu.pk (M.K. Jamil), waqar.ashraf.21@ucl.ac.uk (W.M. Ashraf), syedsaqib@uet.edu.pk (S. Saqib), yfouad@ksu.edu.sa (Y. Fouad).

https://doi.org/10.1016/j.ecmx.2023.100438
Received 6 July 2023; Received in revised form 11 August 2023; Accepted 12 August 2023
Available online 14 August 2023

Table 1
Summary of researchers' work exploring techniques on SI engine performance and emissions with biofuel mixtures.

Author Name and Reference	Fuel Blend	ANN	RSM	BP	BSFC	BTE	CO	CO_2	HC	NO_x
Yücesu et al. [22]	Gasoline, Ethanol, and Methanol	✔	✔	↑	↓	–	–	–	–	–
Simsek et al. [23]	Gasoline, LPG, and Bio Gas	–	–		↑	↑	↓	↓	↓	↑
Najafi et al. [24]	Gasoline, and Ethanol	✔	–	↑	↓	↑	↓	↑	↓	↑
Uslu et al. [25]	Gasoline and I-amyl Alcohol	✔	✔	–	↑	↑	↓	–	↓	↓
Barboza et al. [26]	Gasoline hydrogen peroxide and ethanol	✔	✔	–	–	↑	↓	↑	↓	↓
Palani et al. [27]	Gasoline, ethanol, n-butanol	–	✔	–	↑	↑	↓	–	↓	↑
Yusri et al. [28]	Gasoline and secondary butyl alcohol	–	✔	↑	↑	↑	↓	↑	↓	↓
Kaliyaperumal et al. [29]	Gasoline and Gasohol/Hydrogen	✔	–	–	↑	↑	↓	↑	↓	↑
Yaman et al. [30]	Gasoline and 1-heptanol	–	✔	–	↑	↑	↓	↑	↓	↑

Table 2
E100 and E0's characteristics.

Property	Ethanol	Gasoline
Chemical Formula	C_2H_5OH	C_8H_{12}
Composition (C, H, 0) mass%	52.17, 13.04, 34.78	87%, 13%, 0%
Calorific Value (MJ/kg)	26.7	46
Heat of evaporation (kJ/kg)	904	325
Stoichiometric A/F ratio	9.0	14.7
Oxygen content % mass	34.8%	0%
Density kg/m^3	789	740
Flash Point (°C)	13	−43
Auto Ignition Temperature (°C)	420	270
Solubility in water (ml/100 ml H_20)	Infinitely soluble	Infinitely soluble

Table 3
Test engine facets.

Engine Parameter	Value
Bore(mm)	68
Stroke (mm)	45
Displacement (cm^3)	163
Compression ratio	8.5:1
Net power (kW/rpm)	3.6/3600
Fuel tank capacity (Liters)	3.1
Fuel consumption at constant rated power (Liter/hour) @ 3600 rpm	1.4
Engine Oil Capacity (Liters)	0.6

necessitates a significant investment. Hence, biofuel-powered internal combustion engines (ICEs) are expected to remain noteworthy [10–12]. Nevertheless, optimizing their parameters to comply with emissions regulations, ensure energy security, improve efficiency, and meet consumer expectations poses multifaceted challenges. The SGD 9 (Industry, Innovation, and Infrastructure) is aligned with these challenges, which focuses on sustainable industrialization, innovation, and infrastructure to empower environmental sustainability and economic growth [13–15]. Traditional methods involving precise instruments and costly experimentation are time-consuming. These issues are aligned with SDG 12 (Responsible Consumption and Production) [7,14,16]. Consequently, the development of substitute solutions is a pressing need that supports sustainable consumption and production practices. Computational modeling techniques have been used to identify the relationships between operating parameters and accurately predict numerous characteristics of internal combustion engines (ICEs), such as performance, combustion, and emissions [17]. Among these techniques, artificial neural networks (ANN) and response surface methodology (RSM) have emerged as prominent techniques that make accurate predictions and optimize by utilizing diverse input configurations, respectively [18–20]. Table 1 provides a summary of previous research conducted by various scholars employing different techniques for this purpose. An ANN efficiently handles numerical data with several variables that would be challenging otherwise. In contrast to conventional techniques, a well-trained neural network makes faster predictions, bypassing time-consuming and complex mathematical problem-solving as well as the need for expensive and complex physical and computer models [21].

The performance of SI engines utilizing ethanol-methanol blends was determined by Kapusuz et al. [31]. The study shows that the mixture of 11% methanol and 1% ethanol by volume exhibited improved performance, yielding regression coefficients within the range of 0.931–0.990. Samet et al. [32] developed an ANN model to predict results for a diesel engine fueled with a diethyl ether blend up to 10%, achieving regression coefficients (R2) ranging from 0.964 to 0.9878 and mean relative error (MRE) values ranging from 0.51% to 4.8%. Khandal et al. [33] examined the performance of a diesel engine powered by a mixture of plastic pyrolysis oil, diesel, and ethanol by employing the ANN model. The ANN technique is also utilized by Shivakumar [34] to evaluate engine efficiency and emissions. The performance of the butanol-gasoline based SI engine was predicted by Liu et al. [35]. Moreover, Rezaei et al. [36], conducted a study and established that the ANN model showcased faster convergence and exceptional performance.

Table 1 showcases prior studies optimizing engines based on experimental data, rather than utilizing predicted data. In the present study, the ANN model efficiently predicted output values based on given inputs. These input-predicted output pairs were then optimized using the RSM technique. This integration significantly reduces the number of experimental runs. In scenarios where new, unseen input data is encountered, no longer a need to conduct expensive experiments to obtain corresponding outputs. Instead, the well-trained ANN model accurately predicts the required outputs and the RSM optimization process delivers optimal operating conditions for the engine. The research highlights how the ANN model's architecture influences performance. This methodology aids in identifying the most accurate and robust model for predicting engine operations. By considering a broader range of outputs, the research contributes to a more comprehensive understanding of the engine's operating parameters and opens new possibilities for optimizing engine operations.

The contribution of this research to achieving multiple SDGs simultaneously and fostering a sustainable and resilient future for the planet as a whole makes it distinctive. The integration of two cutting-edge computational techniques (ANN and multi-level RSM) to predict and optimize operations of the ethanol-powered engine offers a deeper comprehension of the complex interactions between fuel blends, engine performance, and environmental impact. This distinctive aspect of this study opens up exciting possibilities for dropping experimental runs and intricate mathematical modeling. The study represents a notable strive for affordable and clean energy, sustainable industrialization, responsible consumption and production, and climate action.

Materials and methods

This section presents the preparation of fuel blends, experimental design for testing, ANN model development, and methods and definitions for RSM-based optimization.

Formulation of fuel blends

In this study, ethanol was sourced from Shahmurad Ethanol Limited,

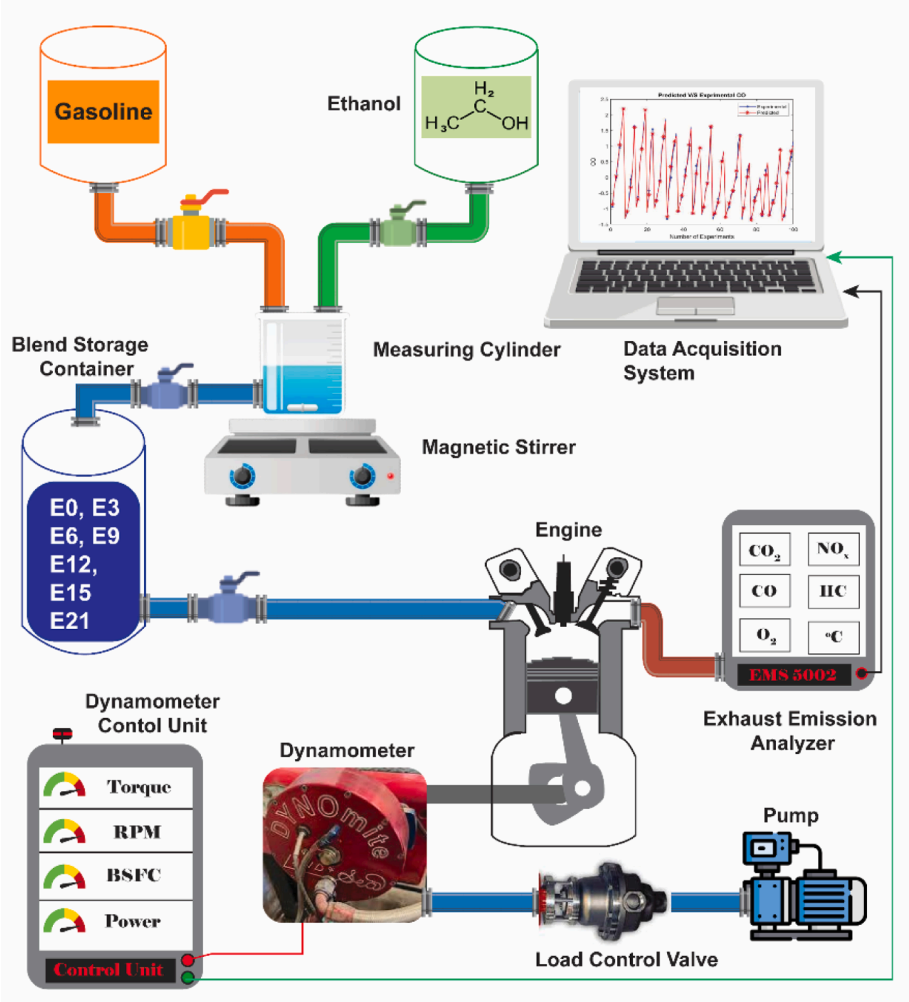

Fig. 1. The layout of the test rig and experimental configuration.

Table 4
Comprehensive testing scheme.

Factors	Description
Fuel	E0, E3, E6, E9, E12, E15, E21
Loads	50% and 100%
Speed range	1300–3700 RPM (with an increase of 300 rpm)
Performance Parameters	Torque, BP, BSFC and BTE
Emission Parameters	CO_2, CO, HC, NOx
Ambient Temperature	27C
Atmospheric Pressure	1 atm

Table 5
Specification of ANN models structures.

Specifications	Description
ANN-1HL-9 N, ANN-1HL-11, ANN-1HL-15 N, ANN-2HL-9 N, ANN-2HL-11 N, ANN-2HL-15 N	The digits designate the number of hidden layers and neurons in the hidden layer
Training Algorithm	Levenberg-Marquardt
Epochs	100
In-Training Performance Plots	Regression and error histograms
Post-training performance parameters	MRE, RMSE, and R^2
Data Distribution	70% Training, 15% (Testing) and 15% (validation)
Stopping Criteria	Minimization of mean square error

a principal ethanol producer in Pakistan, and gasoline was obtained from Pakistan State Oil (PSO). Gasoline was marked as the reference for all the blends. Table 2 outlines ethanol (E100) and gasoline (E0) attributes.

The ethanol was added to gasoline at various concentrations of 0%, 3%, 6%, 9%, 12%, 15%, 18%, and 21% by volume, resulting in fuel blends represented as E3, E6, E9, E12, E15, E18, and E21 respectively. Blends were continuously stirred using a magnetic stirrer for 15 min to ensure a fully homogeneous mixture of the fuels.

Experimental setup and testing plan

An air-cooled spark ignition (SI) engine with an overhead valve was used during this study. Table 3 presents the qualifications of the test engine.

For testing, the engine was connected through a mild steel shaft to a 7-inch Dynomite dynamometer, with a water-brake system. By utilizing EMS-5002 analyzer, emissions were quantified. A 500-ml measuring cylinder (0.5 ml grade) was used to measure fuel flow. The working fluid was water for applying loads through the piping system. The experimental setup schematic is illustrated in Fig. 1.

Data acquisition was accomplished using a system with signal conditioning circuitry to convert sensor signals into digital data. DYNOMAX software measured engine performance, while the emissions measurement system covered a wide range of engine speeds for comprehensive data collection in different operating conditions. The

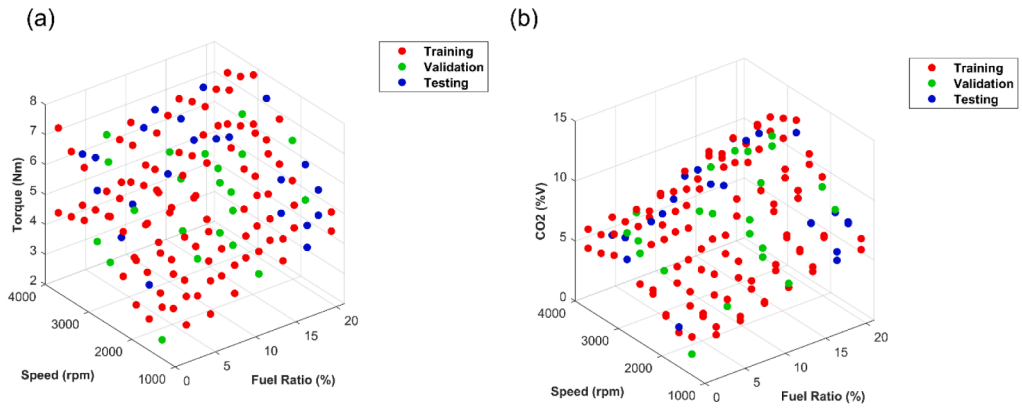

Fig. 2. Random distribution of data set for (a) torque and (b) CO_2.

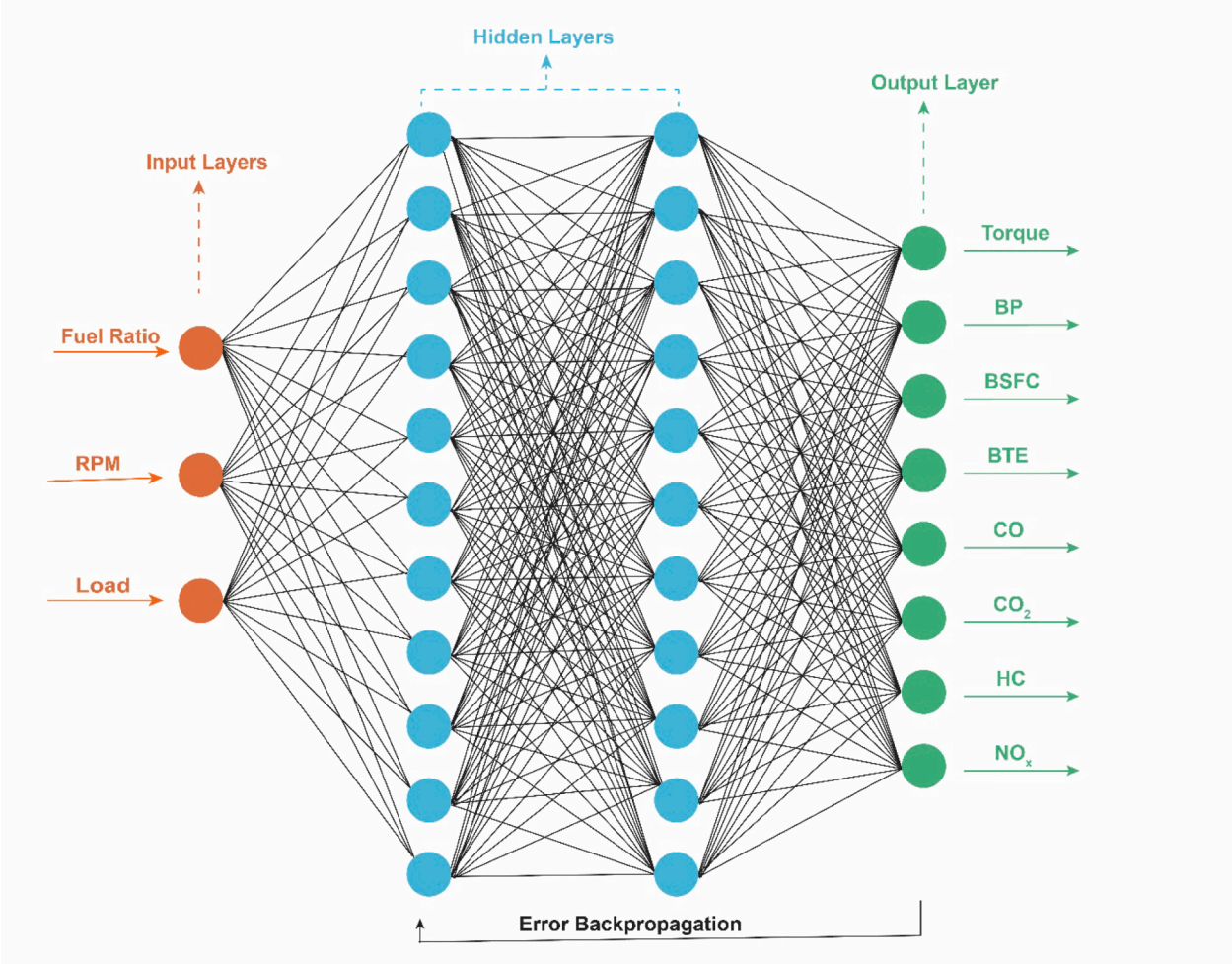

Fig. 3. Structure of ANN-2HL-11 N.

engine testing involved no structural modifications. The engine speed was progressively increased from 1300 rpm to 3700 rpm in 300 rpm increments, with 50% and 100% loads applied. The steady-state operation was achieved using gasoline as the initial fuel. Blends were prepared shortly before testing to maintain consistency and prevent moisture accumulation. Three repetitions of each test were executed to gauge its accuracy, and average readings were recorded. Dynomite 2010 software accurately recorded speed and load values. Fuel consumption, BSFC, BP, and BTE were calculated using heating values and density. Table 4 summarizes the testing scheme. (See Fig. 1.)).

Development of ANN models

Using MATLAB software for formulating and executing ANN models offers several strengths and benefits [37]. The gathered dataset from the data acquisition system includes fuel ratio, load, RPM, torque, BP, BSFC,

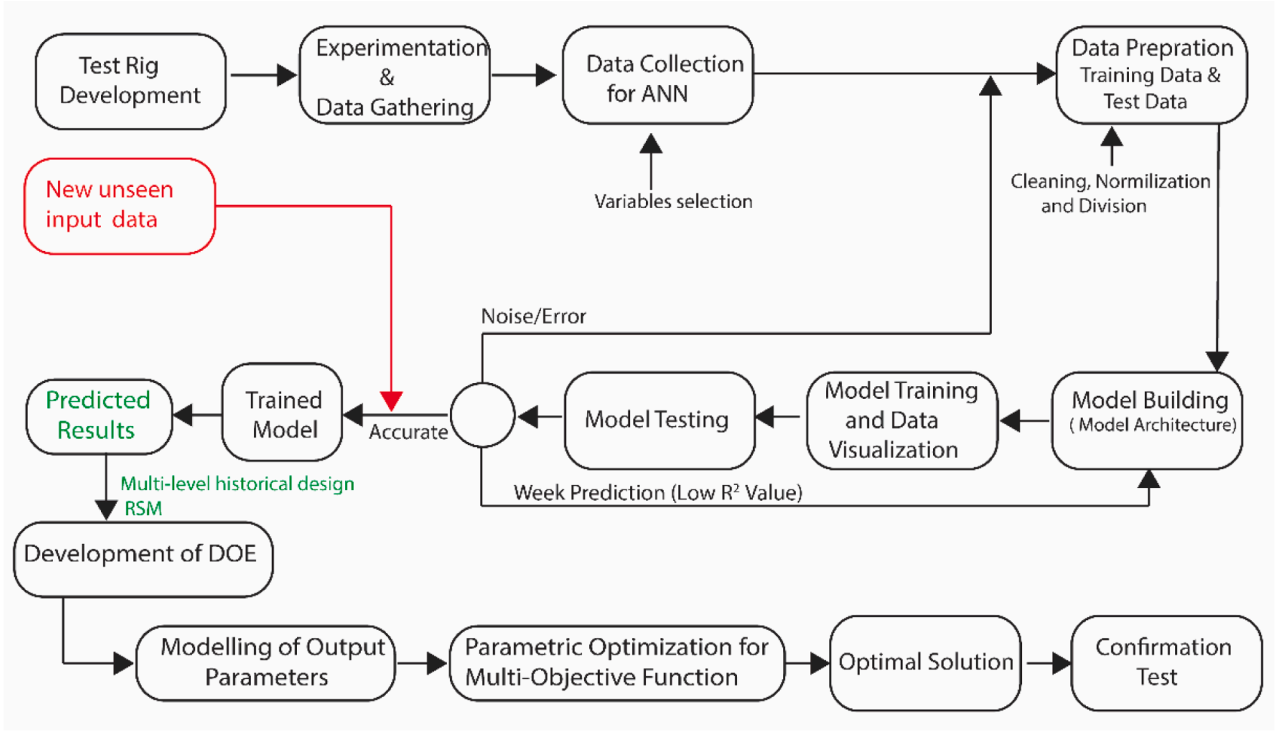

Fig. 4. Flow chart for the methodology of ANN-integrated RSM.

Table 6
Model defining parameters.

Numeric Factor		Units	Subtype	Low Level	High Level	Mean	Std. Dev.
A	Load	%	Continuous	50	100	75	25.09
B	Speed	rpm	Continuous	1300	3700	2500	777.3
C	Fuel Ratio	%	Continuous	0	21	10.50	6.69

Table 7
R^2 for responses given by ANOVA.

Response	Adjusted R^2	Predicted R^2
Torque	0.9379	0.9332
BP	0.9797	0.9774
BTE	0.7220	0.7107
BSFC	0.6585	0.6437
CO	0.9646	0.9624
CO_2	0.7929	0.7851
HC	0.9255	0.9188
NO_x	0.9730	0.9707

BTE, CO, CO_2, HC, and NOx concentration. With a standard deviation of 1 and a mean of 0, the dataset was transformed by executing the 'zscore' argument in the z-score normalization. It ensures that all input features have equal weights during training. The transformation can shift the original range of values to include negative values or values greater than the original maximum. Z score for a data point is given by equation (1).

$$Z = \frac{(X - \mu)}{\sigma} \tag{1}$$

where X is the original value, μ is the mean of the data, and σ is the standard deviation. The connectivity and structure of an ANN model are dictated by its architecture [38,39]. Table 5 outlines the initial six different structures that were established and trained in the study. The 144 sets of experimental data were segregated into three distinct groups in this study. To facilitate the random selection of data points, the 'divideind' function was utilized to divide the data as 70% (100/144) for training, 15% (22/144) for validation, and 15% (22/144) for testing. To ensure an unbiased evaluation of the model's performance and the trained model's generalizability, the data must be carefully divided into these sets. The random distribution of the data set for torque and CO_2 is shown in Fig. 2. The trainlm function was employed for training, signifying the use of the Levenberg-Marquardt algorithm [40]. This algorithm empowers the effective handling of non-linear problems and rapid convergence by combining the benefits of the Gauss-Newton and

Table 8
P-values of model terms.

Response	A	B	C	AB	AC	BC
Torque	<0.0001	<0.0001	<0.0001	0.0095	0.0104	<0.0001
BP	<0.0001	<0.0001	<0.0001	<0.0001	0.8123	<0.0001
BTE	<0.0001	<0.0001	0.0073	–	–	–
BSFC	<0.0001	<0.0001	0.0196	–	–	—
CO	<0.0001	<0.0001	<0.0001	<0.0001	<0.0001	0.6472
CO_2	<0.0001	<0.0001	<0.0001	–	–	–
HC	<0.0001	<0.0001	<0.0001	0.041	<0.0001	0.0187
NOx	<0.0001	<0.0001	<0.0001	0.5922	<0.0001	0.0002

A = Fuel ratio B = Engine load C = RPM

Table 9
Performance metrics of ANN structures for each output.

Output	*Performance Parameters*	*ANN Models Nomenclature*					
		ANN-1HL-9 N	ANN-1HL-11 N	ANN-1HL-15 N	ANN-2HL-9 N	ANN-2HL-11 N	ANN-2HL-15 N
Torque	R^2	0.99292	0.99415	0.99554	0.99560	**0.99594**	0.99537
	RMSE	0.11553	0.10089	0.09539	0.09821	0.09177	**0.08847**
	MRE	−0.03516	−0.02924	−0.01398	−0.01616	**−0.03198**	−0.00464
BP	R^2	0.99292	0.99415	0.99554	0.99560	**0.99594**	0.99537
	RMSE	0.11553	0.10089	0.09539	0.09821	**0.07177**	0.08847
	MRE	−0.03516	−0.01924	−0.01398	−0.01616	**−0.03198**	−0.00464
BSFC	R^2	0.99526	0.99484	0.99524	0.99565	**0.99596**	0.99541
	RMSE	1.79753	**1.67847**	1.77320	1.79918	1.81497	1.68845
	MRE	0.11166	0.00143	−0.10810	0.17326	**−0.80373**	0.83854
BTE	R^2	0.99373	0.99065	0.99234	0.99383	**0.99456**	0.99193
	RMSE	0.11524	0.13483	0.12218	0.11056	**0.10001**	0.12263
	MRE	0.40082	0.36798	−0.04032	0.44777	**−0.13693**	0.46470
CO	*R*	0.99024	0.99391	0.99460	0.99389	**0.99653**	0.99406
	RMSE	0.14089	0.11364	**0.09876**	0.10496	0.09897	0.09984
	MRE	0.86602	0.61949	−0.32298	**−0.71277**	−0.27307	−0.19510
CO_2	R^2	0.98600	0.98872	0.98925	0.99211	**0.99504**	0.98386
	RMSE	0.16756	0.14854	0.12987	0.13083	0.14154	**0.11318**
	MRE	0.65879	0.37526	0.29761	0.43750	**0.03063**	0.46725
HC	R^2	0.99353	0.98812	0.99432	0.99606	**0.99709**	0.99318
	RMSE	0.11490	0.14961	0.10801	0.08963	**0.07541**	0.10987
	MRE	0.00968	0.02983	0.06622	**−0.02307**	0.02929	0.03305
NOx	R^2	0.99507	0.99501	0.99589	0.99587	**0.99669**	0.99001
	RMSE	0.09964	0.10013	0.09327	0.08748	**0.07533**	0.08378
	MRE	0.15185	0.14952	**0.03383**	0.20429	0.17002	0.26562

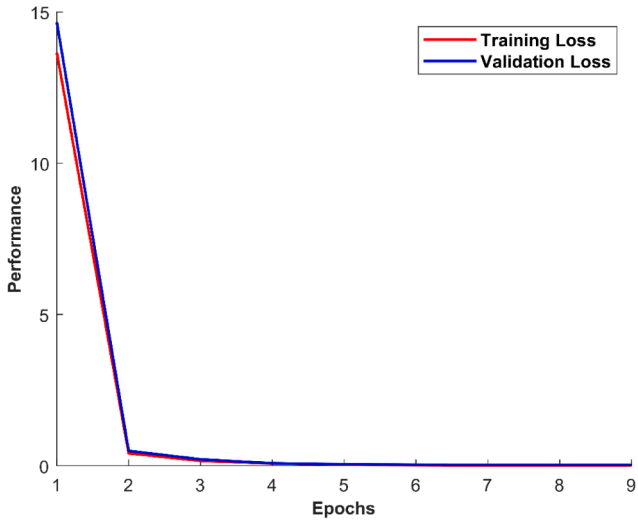

Fig. 5. Learning curves of the ANN-2HL-11 N model.

gradient descent methods. The ReLU (Rectified Linear Unit) activation function was employed, while sigmoid and tanh are also commonly used for similar problems [25,41–43]. Fig. 3 presents the structure of an ANN model consisting of two hidden layers with 11 neurons in each layer. A loss function was employed to compute the prediction error. The error was then propagated backward through the network by executing the backpropagation algorithm. Weights and biases were adjusted based on the gradient of the loss function concerning these parameters.

The adjusted weights and biases were then updated in each iteration using the optimization algorithm Adam. RMSprop is also well known [40,44]. By computing performance metrics such as R^2 (coefficient of determination), MSE, and RMSE, the consistency and precision of the models were quantified. An ANN model with a complex structure starts to memorize the training data instead of learning patterns (overfitting), and an ANN model with a structure that is not complex enough to capture the underlying pattern in the data leads to underfitting. Both problems have a negative influence on performance. In this study, learning curves are plotted to check whether the model is overfitted, underfit, or a good fit. Once the ANN model was acceptable, engine performance and emissions were forecasted for unobserved data. By comparing the forecasted results with experimental values, the model's dependability was confirmed.

RSM methodology approach

The current study is aimed at utilizing an ANN model to predict the optimal ethanol ratio, engine load, and speed and to attain efficient performance and reduced emissions. To accomplish this, the study incorporates RSM through Design-Expert version 13 was used for defining the multi-level historical design. Fuel ratio, engine load, and RPM were chosen as continuous numeric factors, while ANN estimated values of torque, BP, BTE, BSFC, CO, CO_2, HC, and NO_x were nominated as response variables. Fig. 4 presents a graphical understanding of the innovative methodology for this integration. The model-defining parameters are listed in Table 6.

The model attributes were evaluated by applying analysis of variance (ANOVA). A significance benchmark of a p-value less than 0.05 was used. Given the null hypothesis's validity, the p-value signifies the probability of seeing test results as extreme as the observed ones. [25,45–47]. The ratio of squared deviations to individual sums of squares (SOS) was employed to compute the percentage contribution (PC%) of each model term. The F-value, a test statistic in ANOVA, specifies the overall worth of mean differences between groups. A large F-value suggests significant differences among group means if it exceeds the critical value [28].

The predicted R^2, a reasonable agreement between the predicted and adjusted R^2, and the p-value determine the selection of an appropriate model. R^2 values close to 1 specify a perfect linear curve. R^2 values from the ANOVA test are listed in Table 7, signifying good model fit and agreement with experimental data.

Table 8 provides insights into the significance of factors in the responses based on their corresponding p-values. At 95% confidence level, the study was carried out. By analyzing the p-values presented in Table 8, it becomes evident that the ethanol ratio, engine speed, and load have significant effects on all the responses.

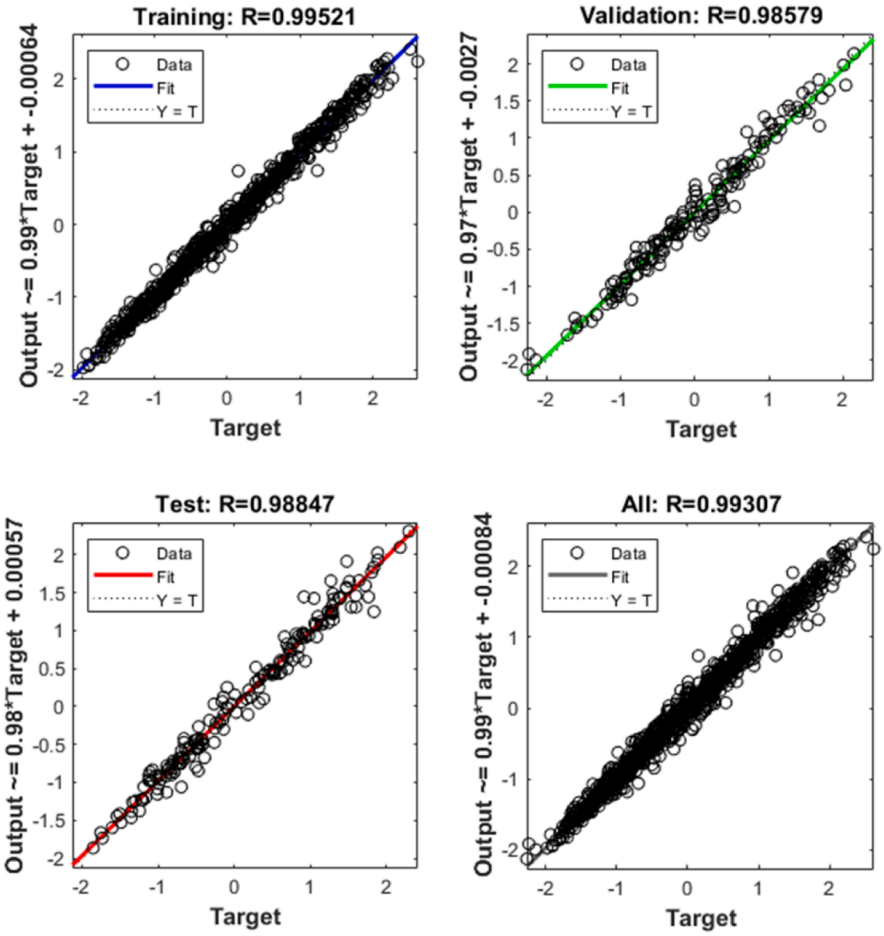

Fig. 6. Regression plots of the ANN-2HL-15 N model.

3 Results and discussions

This section presents the performance results of the ANNMs (ANN models), the prediction outcomes derived from the trained model, and the optimized results achieved using RSM.

Annms performance results

The ability of an ANN model to capture the complex relationships in the data has a significant dependence on the number of hidden layers and neurons. An ANN model with a complex structure starts to memorize the training data instead of learning patterns (overfitting), and an ANN model with a structure that is not complex enough to capture the underlying pattern in the data leads to underfitting. Both problems have a negative influence on performance. Table 9 presents three key metrics to evaluate each model's performance. The bold values are desired values, aiding in identifying the best-performing model.

Learning curves are shown in Fig. 5 which shows moderately high initial training and validation loss. The loss steadily declines and reaches a plateau when more training and validation instances are added.

A well-fitted model is indicated by the proximity of training and validation losses, with validation somewhat greater. This result emphasizes the significance of finding the right balance between model complexity and the capacity to generalize patterns from the data, avoiding both overfitting and underfitting and ultimately resulting in enhanced performance. Based on the regression plot, shown in Fig. 6 data points tend to cluster around the diagonal line and the ANN-2HL-11 N model achieves high R values of 0.99521 (training), 0.98579 (validation), 0.98847 (testing), and 0.99307 overall. This shows that the ANN-2HL-11 N model accurately captures underlying patterns and relationships, which reinforces its performance.

Predicted outputs were plotted against experimental values to thoroughly evaluate the performance and accuracy of the trained model. In Fig. 7(a) the model's performance throughout the training process is assessed for torque. These randomly selected 100 data points are the part of training set which is 70% (100/144) of the available dataset. The focus is on the relative position of predicted and experimental values of each experiment. Each experiment was performed for a different set of conditions. Therefore, there is no physical relationship between the variable values and the increasing number of experiments in this figure. The negative values of torque that were initially below the mean of the dataset are the result of Z-score normalization. Instead of focusing on the absolute values themselves, this shift towards negative values is more about the relative positions and distributions of the normalized data. The predicted and experimental values of torque for each experiment are closely located in Fig. 7 (a) which is graphical evidence of the performance metrics of ANN-2HL-11 N presented in Table 9. Once the ANN model was fully trained, Fig. 7 (b), displays the actual predicted and experimental values following reverse normalization. The entire data set of torque is clustered along a diagonal line (45 degrees). Fig. 7(c and d) presents similar trends for BP. Performance for BSFC, BTE, and emissions is assessed in Figs. 8, 9, and 10 respectively.

In these plots, the negative values for the BP, BTE, BSFC, and emissions are not interpreted as practically or physically negative values. Instead, they show how the normalized data points are positioned about the dataset's original mean. It is important to note that these plots aim to

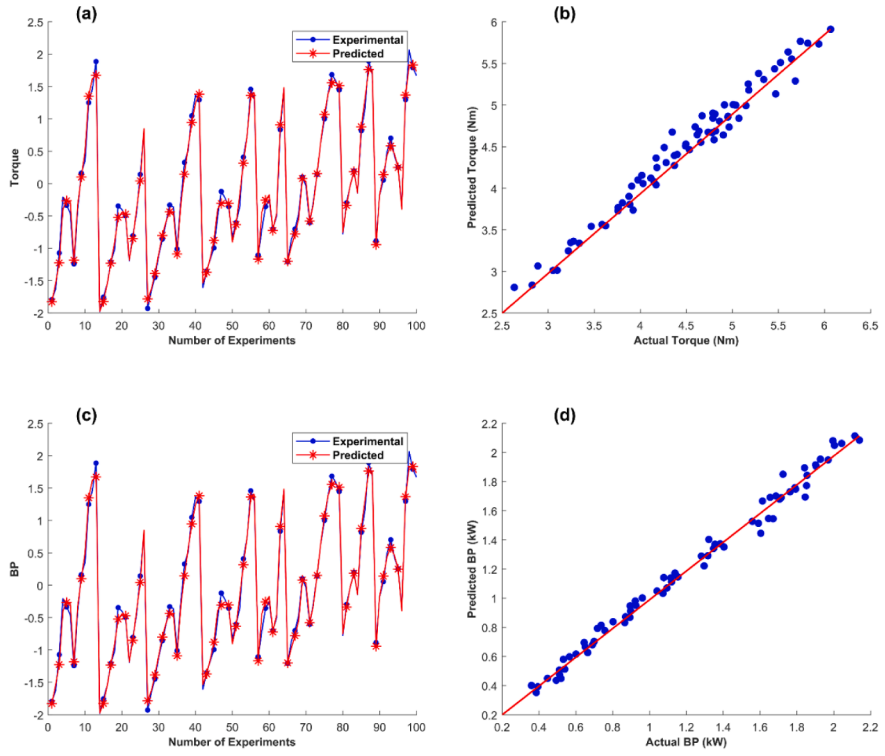

Fig. 7. Predicted values in comparison with experimental values of (a) normalized, and (b) actual torque dataset and, (c) normalized and (d) actual BP dataset.

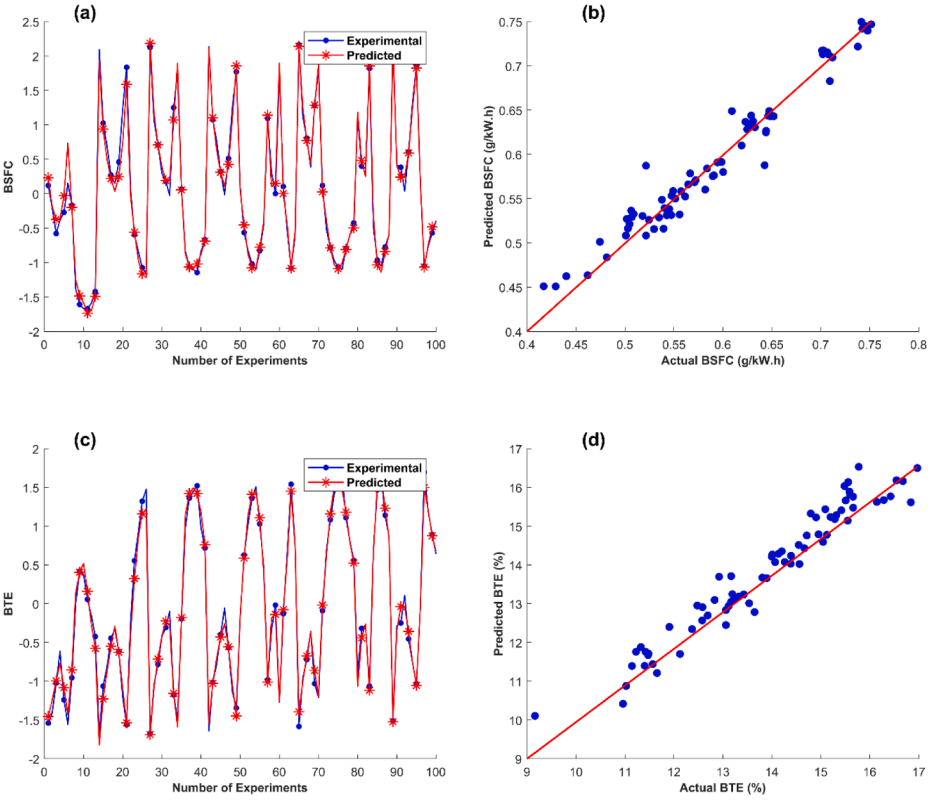

Fig. 8. Predicted values in comparison with experimental values of (a) normalized and (b) actual BSFC dataset, and (c) normalized, and (d) actual BTE dataset.

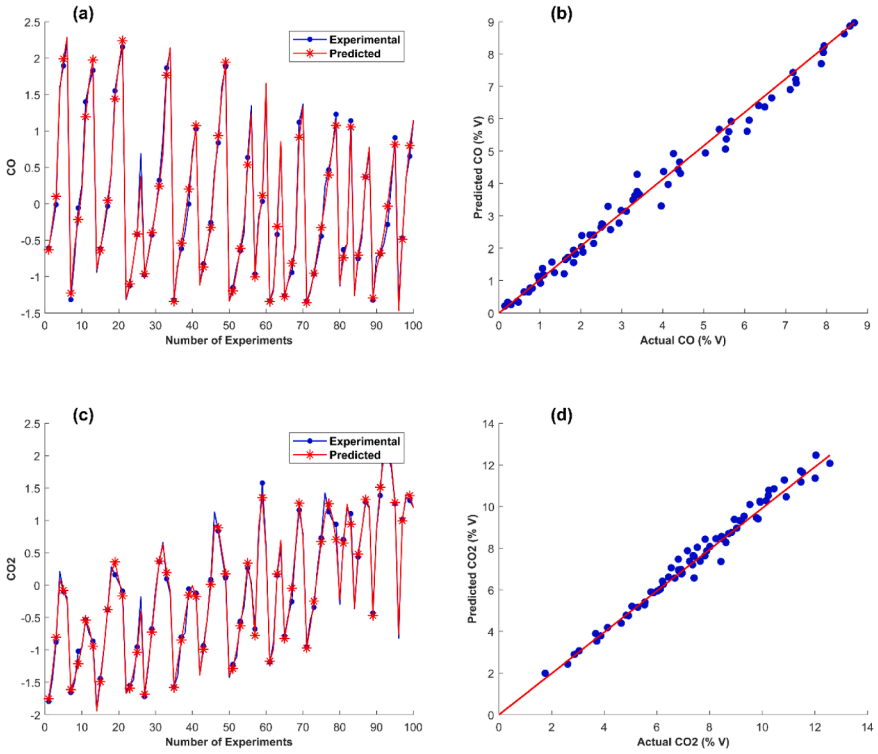

Fig. 9. Predicted values in comparison with experimental values of (a) normalized and (b) actual CO dataset, and (c) normalized, and (d) actual CO_2 dataset.

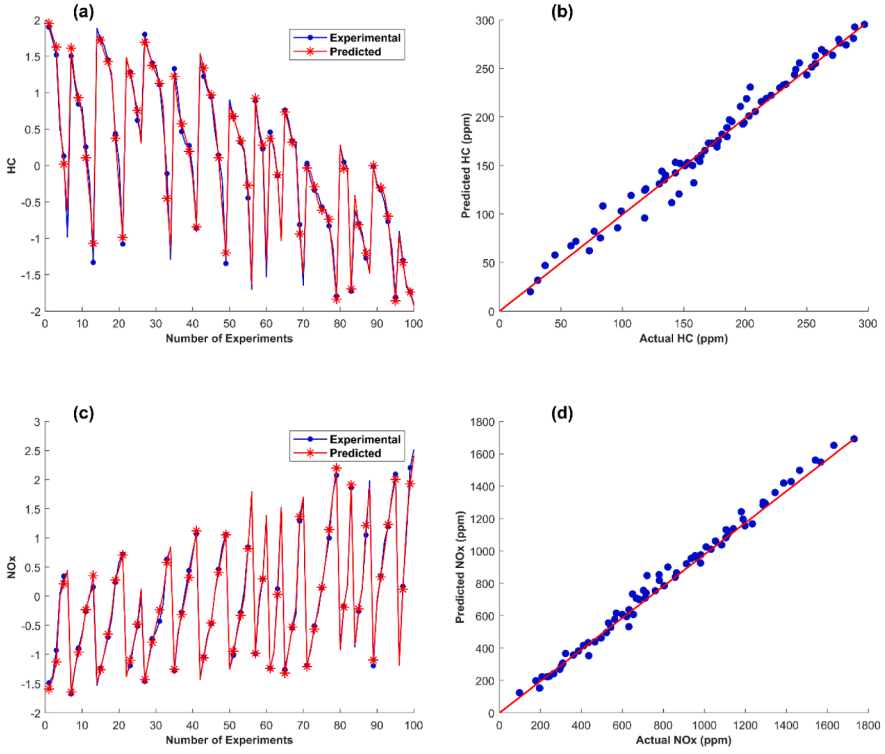

Fig. 10. Predicted values in comparison with experimental values of (a) normalized, and (b) actual HC dataset, and (c) normalized, and (d) actual NOx dataset.

Table 10
Setup for optimization.

Variable	*Optimization Criteria*	*Lower Limit*	*Upper Limit*	*Importance*	*Lower Weight*	*Upper Weight*
A: Fuel Concentration	is in range	0	21	3	1	1
B: Load	is in range	50	100	3	1	1
C: RPM	is in range	1300	3700	3	1	1
Torque	is in range	2.631	7.71142	3	1	1
Brake Power	maximize	0.35863	3.22758	3	1	1
BSFC	minimize	0.30895	0.75138	3	1	1
BE	maximize	9.15977	22.4894	3	1	1
CO	is in range	0.0707	8.68	3	1	1
CO_2	is in range	1.75	12.57	3	1	1
HC	minimize	18.53	297	3	1	1
NOx	is in range	97	1911.86	3	1	1

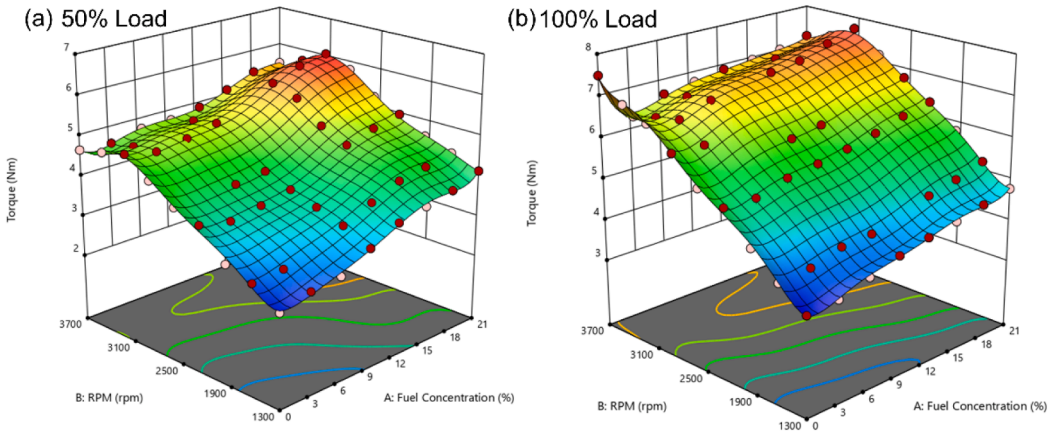

Fig. 11. Surface analysis of torque at (a) 50% load and at (b) 100% load.

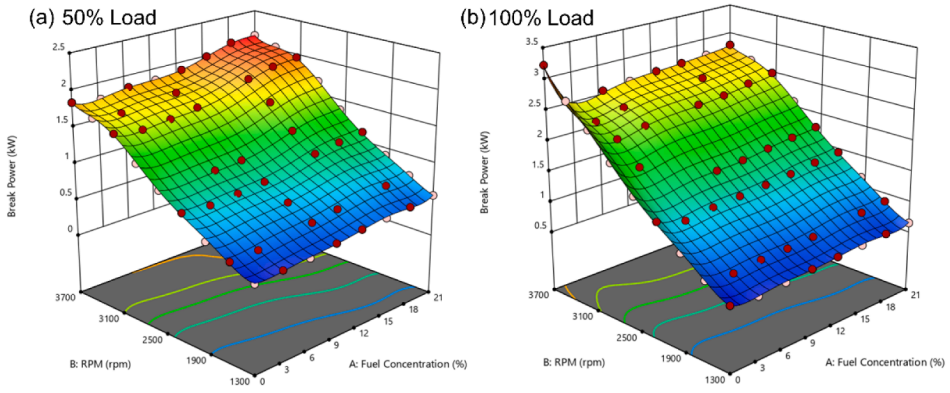

Fig. 12. Surface analysis of BP at (a) 50% load and at (b) 100% load.

highlight the predictive model's consistency in capturing trends and overall behavior. The close alignment between predicted and experimental values within the expected error range reaffirms the effectiveness of the model.

Rsm-based optimization results

To optimize the engine, BSFC, emissions, BTE, and BP were to be minimized and maximized while keeping all study factors within-range criterion. Table 10 demonstrates the defined limitations and optimization arrangement. Optimal model fitting and interpretation of the results depends on "Weight" and "Importance" in RSM. The weight allows for proper consideration of the variability and reliability of experimental data, while the importance helps identify the critical factors driving the response variable. By providing valuable insights into the relationship between factors and responses, they contribute to the robustness and effectiveness of the RSM analysis.

In Fig. 11, the engine demonstrates lower torque output at 1300 rpm, attributed to reduced power generation at lower speeds, known as the "low-end torque" region. As RPM increases beyond this range for all fuel blends in the study, torque output consistently rises. It is attributed to enhanced energy input and output due to the faster burning of fuel at higher speeds [48,49]. At 100% load (Fig. 11(b)), the engine reaches its peak torque region around 3100 rpm, resulting in a 7.7 Nm for E21. However, beyond this region, as RPM continues to increase, torque output declines, known as the "fall-off" or "decline" in torque. As the engine encounters limitations in terms of intake flow, cylinder filling, frictional losses, valvetrain operation, exhaust backpressure, and

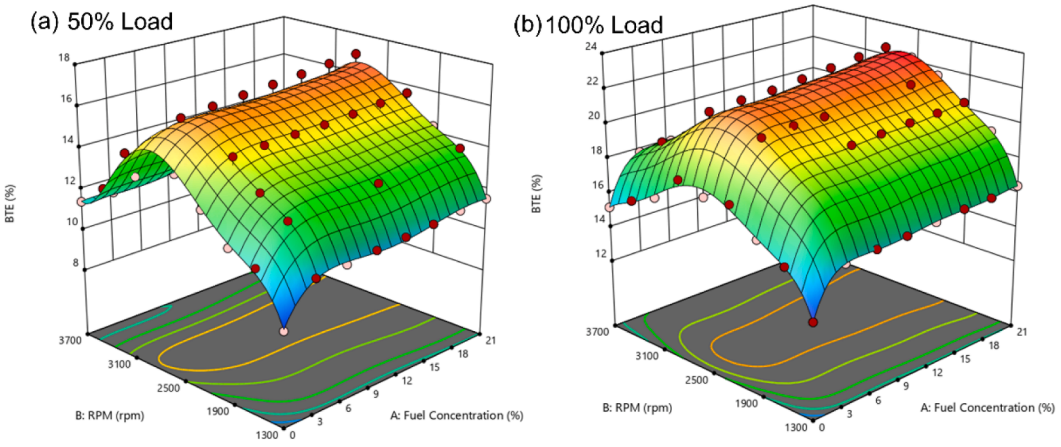

Fig. 13. Surface analysis of BTE at (a) 50% load and at (b) 100% load.

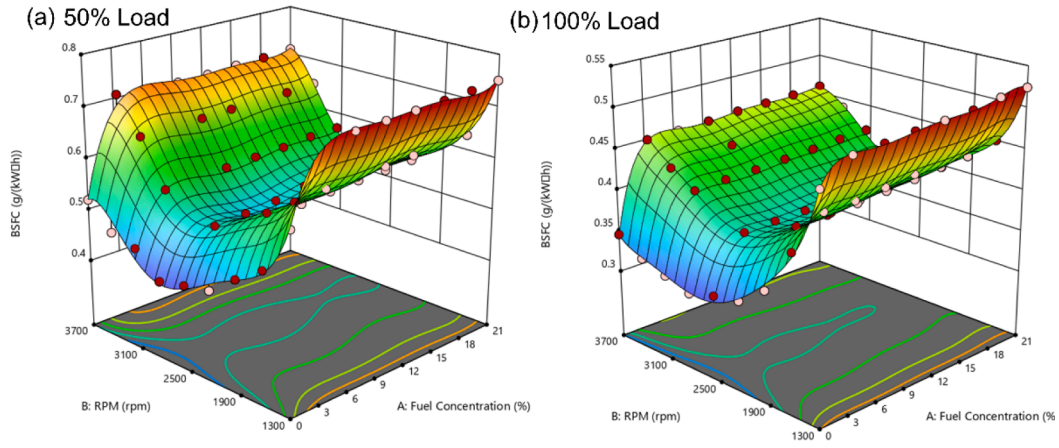

Fig. 14. Surface analysis of BSFC at (a) 50% load and at (b) 100% load.

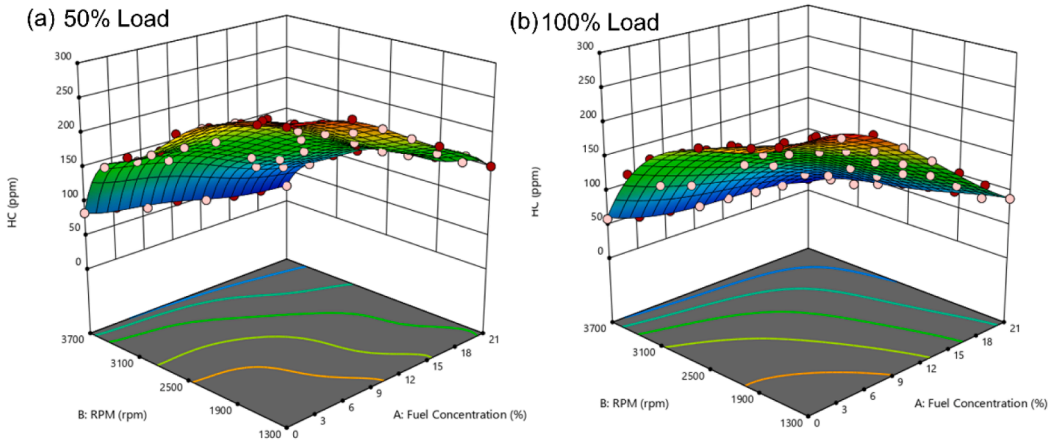

Fig. 15. Surface analysis of torque at (a) 50% load and at (b) 100% load.

mechanical stress [50]. The ethanol ratio consistently increases torque, attributed to ethanol's higher-octane rating, better air–fuel mixture, cooling effect, and ability to achieve higher compression ratios. Increasing the ethanol ratio from 0% to 21% at 100% load and 3100 rpm, resulted in a 16.86% increase in torque.

In Fig. 12, it can be observed that at lower speeds, the engine demonstrates a comparatively lower BP. By increasing the RPM to a specific range, the BP increases. Enriching ethanol increases density, smooths combustion (due to oxygen), and boost BP, but higher concentrations decrease calorific value and BP [51]. Maximum brake was observed for increasing the ethanol ratio from 0% to 18% at 100% load and 3100 rpm, which resulted in a 23.70% increase in BP.

Fig. 13 demonstrates that the BTE increases within a specific RPM range, reaching its highest value of 22.49% at 2800 rpm and 100% load

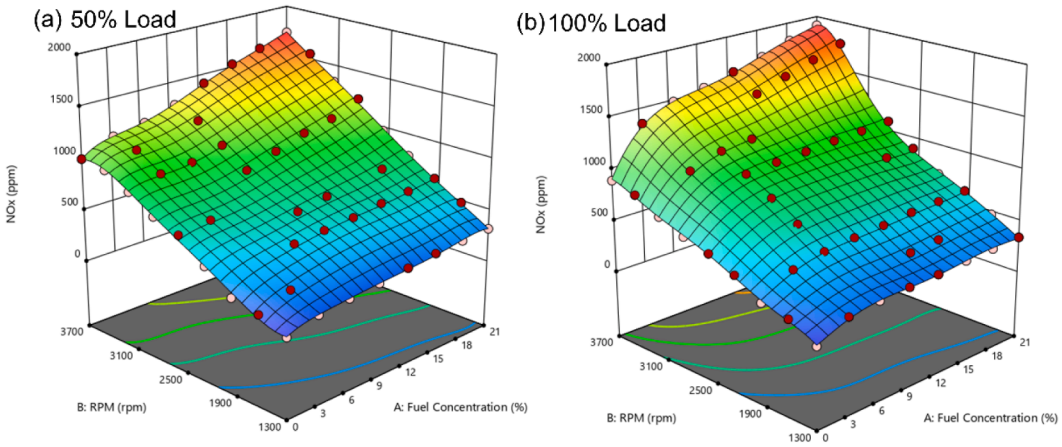

Fig. 16. Surface analysis of torque at (a) 50% load and at (b) 100% load.

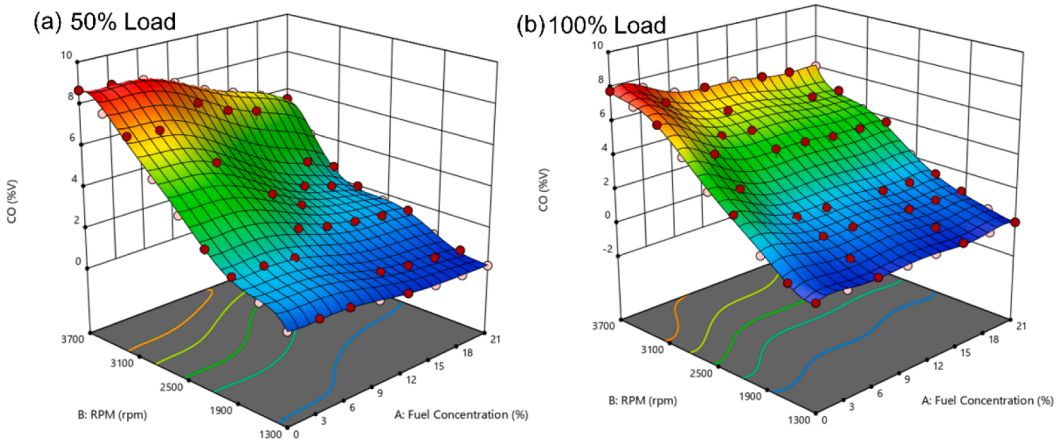

Fig. 17. Surface analysis of CO at (a) 50% load and at (b) 100% load.

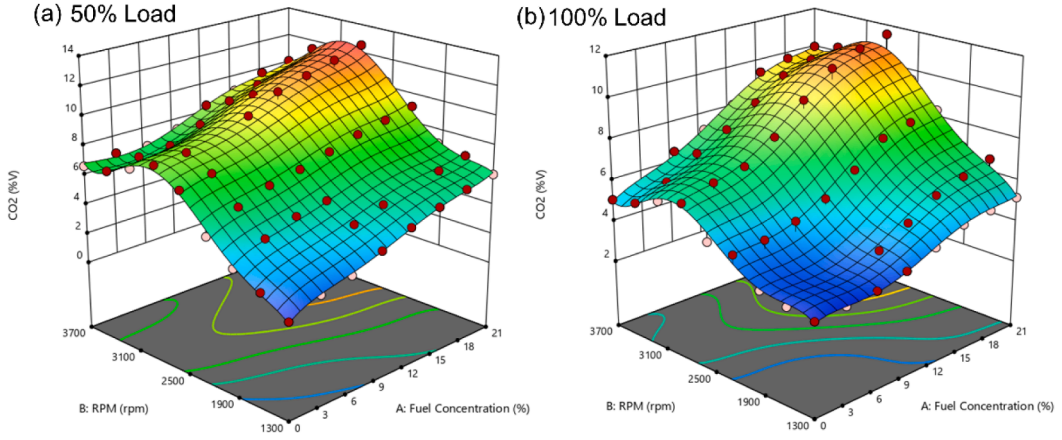

Fig. 18. Surface analysis of CO_2 at (a) 50% load and at (b) 100% load.

for E21. Increasing the engine speed from 1300 rpm to 2800 rpm leads to a significant 26.8% improvement in BTE. However, BTE starts to decline at speeds above 2800 rpm. Lean mixtures at lower speeds increase BTE, but faster and abrupt combustion at higher speeds decreases BTE [27]. BTE shows an upward trend with higher ethanol ratios, especially when the ratio rises from 0% to 6%, resulting in a higher-octane rating and compression ratio and increased BP and BTE.

In Fig. 14, the BSFC initially decreases as RPM increases within a specific range, but beyond that range, it starts to rise. Lower speeds result in a decrease in BSFC due to a substantial increase in BP. However, at higher speeds, the swift and unexpected combustion leads to a rapid increase in BSFC [52]. For instance, increasing the engine speed from 1300 rpm to 2800 rpm at 100% load for E3 led to a 26% decrease in BSFC. At speeds higher than 2800 rpm, BSFC began to increase. The

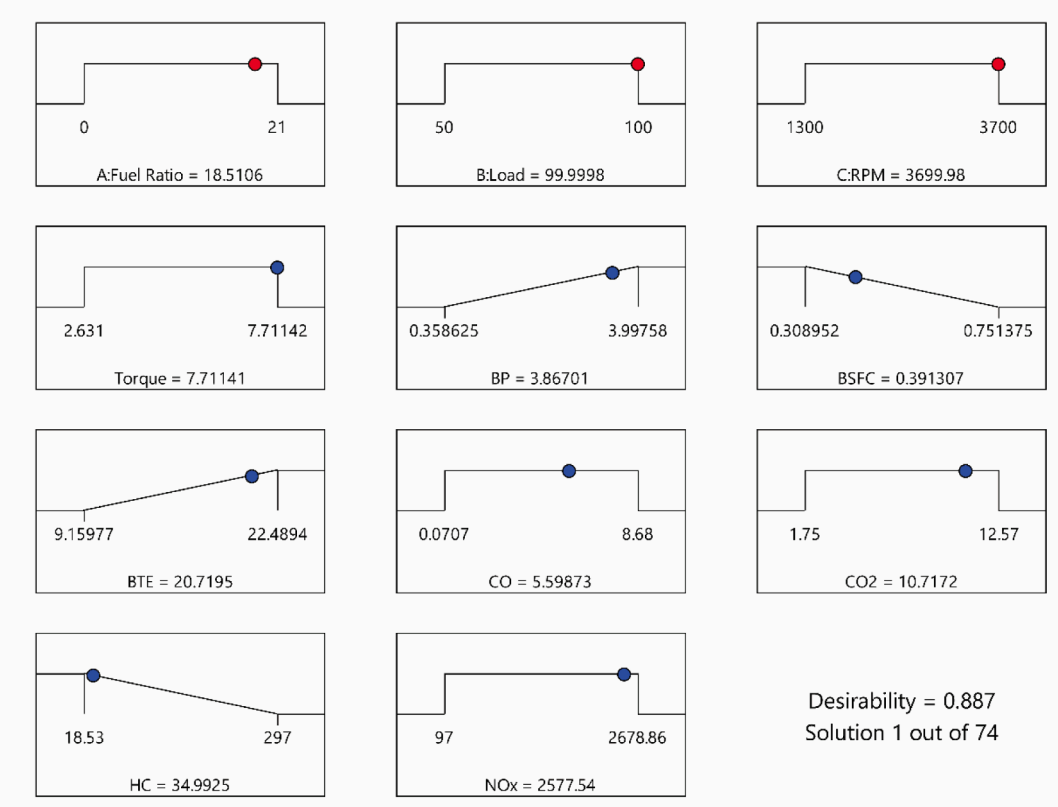

Fig. 19. Ramp chart displaying the optimal operational parameters for the engine.

Table 11
Results of the confirmation test.

	Torque	BP	BTE	BSFC	CO	CO_2	HC	NO_x
Optimized Value	7.71	3.87	20.72	0.391	5.6	6.01	34.99	2577.5
Test Value	7.92	3.99	21.24	0.379	5.8	6.23	33.69	2489.9
Error (%)	2.8	3.3	2.5	3.1	3.5	3.6	3.7	3.4

Table 12
Outputs comparison at optimal operating conditions with pure gasoline fuel.

	Torque (Nm)	BP (kW)	BTE (%)	BSFC (kg/kW.h)	CO (% V)	HC (ppm)	NO_x (ppm)
E0	7.0	3.23	15.96	0.346	7.79	58.41	1819
E18.5	7.71	3.87	20.72	0.391	5.6	34.99	2577.5
% Difference	9.4	19.9	29.8	12.9	− 28.1	− 40.1	41.7%

Table 13
Assessment of ANN and RSM model performances.

	ANN			RSM		
	R^2	MRE	RSME	R^2	MRE	RSME
Torque	0.9959	−0.0319	0.0917	0.9162	−0.0345	0.0991
BP	0.9959	-0.0717	0.0319	0.9063	-0.0782	0.0348
BSFC	0.9959	-1.8149	0.8037	0.9162	-1.9601	0.8680
BTE	0.9945	-0.1000	0.1369	0.8951	-0.1100	0.1506
CO	0.9965	-0.0989	0.2730	0.8669	-0.1118	0.3085
CO_2	0.9950	0.1415	0.0306	0.8855	0.1571	0.0339
HC	0.9970	0.0754	0.0292	0.8973	0.0829	0.0322
NOx	0.9966	0.0753	0.1700	0.9867	0.0760	0.1717

lowest BSFC value occurred at 2800 rpm and 100% load. Moreover, increasing the ethanol ratio from 0% to 21% at 100% load and 2800 rpm resulted in a 19.5% increase in BSFC. The increase in BSFC is due to ethanol's lower energy content and different stoichiometric air–fuel ratio requirements compared to gasoline and its altered combustion characteristics [53–55].

A reduction in HC concentration is shown in Fig. 15 as the ethanol ratio and RPM increase. The lowest recorded HC value of 8.53 ppm occurred at 3700 rpm and 100% load for E21. This can be attributed to the higher oxygen content in the fuel, resulting in a relative increase in the air–fuel ratio (AFR) and subsequently reducing HC emissions. When the engine speed increased from 1300 rpm to 2800 rpm and the fuel ratio changed from E0 to E21, there was a significant reduction of approximately 46.31% in HC concentration. Fig. 16 demonstrates an increase in NO_x concentrations as the ethanol ratio and RPM increase. The level of NOx emissions is influenced by exhaust temperature, which escalates with load and speed [56]. It is evident that as the ethanol content in the fuel rises, so does the emission of NOx. Accelerated fuel combustion leads to higher flame temperatures, contributing to increased NOx [57,58].

Increasing the ethanol concentration in the gasoline-ethanol blend, as depicted in Fig. 17, leads to a noticeable decrease in CO emissions [59,60]. This is attributed to improved combustion completeness and a shift towards a stoichiometric air–fuel ratio. At 1300 rpm and 100% load, the lowest CO emission was observed for E21, with a significant reduction of 32.21% when the ethanol ratio increased from 0% to 21%. Fig. 18 shows that lower RPMs result in lower CO_2 emissions due to reduced fuel consumption at lower power outputs. As RPM increases, CO_2 emissions rise as the engine operates at higher power outputs, leading to increased fuel consumption. However, beyond 2800 rpm, engine efficiency decreases, leading to reduced fuel consumption and lower CO_2 emissions.

Fig. 19 illustrates ramp chart displaying the optimal operational parameters for the engine. The optimal operating conditions for the engine were determined to be an ethanol volume fraction of 18.5%, an engine speed of 3699.9 rpm, and a 100% load setting.

Under these conditions, the engine exhibited favorable performance and emission characteristics, including torque of 7.71 Nm, BP of 3.87 kW, BSFC of 0.391 kg/kW.h, BTE of 20.72%, and low emissions of CO (5.6 % V), CO_2 (10.71 % V), HC (34.99 ppm), and NOx (2577.5 ppm). The calculated composite desirability (D) value of 0.887 validates the optimized model, indicating that the engine responses have been accurately optimized. Operating the engine at the identified parameters would yield the most desirable results, aligning with the objectives of the study. Experimental verification of the optimized results was conducted through a confirmation test and results are summarized in Table 11.

The outputs comparison for the engine running at 3700 rpm, 100% load, and 18.5% ethanol at the same speed and load condition but purely fueled with gasoline is shown in Table 12. The positive values indicate a percentage increase and a negative sign indicates a percentage reduction. The performance matrices between ANN and RSM are compared in Table 13. The ANN model exhibits high R2, low MRE, and RSME than RSM.

Conclusion

The ANN-2HL-15 N model was considered the best model among the six trained models. The model demonstrated exceptional efficiency, with high R^2 values of 0.9952 (training), 0.98579 (validation), 0.98847 (testing), and 0.99307 (overall). It also exhibited the lowest RMSE and MSE values and provided accurate predictions within the range of actual experimental results. The MRE ranged from 0.047% to 0.40%. These results highlight the ANN model's potential for precisely predicting operational effectiveness and discharge levels in small-scale single-cylinder SI engines. The predicted operational parameters and the discharged pollutants were then optimized by integrating a multi-level historical design of RSM.

An ethanol volume fraction of 18.5 %, engine speed of 3700 rpm, and 100% load were identified as optimal operating conditions. Noteworthy improvements resulted from applying these conditions compared to running the engine on gasoline. Specifically, BP and BTE increased by 19.9%, and 29.8%, respectively. Additionally, CO, and HC emissions experienced substantial reductions of 28.1%, and 40.6%, respectively. The increased oxygen and hydrogen content in the blend led to improved combustion, resulting in higher heat generation and elevated emission gas temperatures. Therefore 41.7% increase in NOx emissions was observed. As the test results and optimized values are closely associated, this research has affirmed its resilience for forecasting and optimizing.

The results of this study, which looks at the emissions and performance of the ICE fueled by ethanol, are in line with SDGs 7 and 13. Regarding optimization and prediction, the distinctive combination of ANN and RSM encourages sustainable industrialization, more conscientious consumption, and more ethical production patterns. All these are crucial components of SDGs 9 and 12. To make refined decisions and achieve improved performance and emissions, this research can benefit engine producers and researchers. This alliance between scholars and industry stakeholders supports SDG 17 (Partnerships for the Goals), which also encourages knowledge-sharing to advance the SDGs as a whole.

For future research, dynamic model adaptation has the potential to enhance the capabilities of the established ANN model for ethanol-powered ICEs. Dynamic optimization of such ICEs by utilizing a real-time monitoring and control system along with an ANN predictive model can further enhance performance and reduce emissions. It reinforces the significance of the study by including varying conditions in transient states for the optimization process. Efficiency can be enhanced further by powertrains that combine ethanol utilization with electric energy.

CRediT authorship contribution statement

Muhammad Usman: Conceptualization, Validation, Writing – review & editing, Supervision. **Muhammad Kashif Jamil:** Conceptualization, Methodology. **Waqar Muhammad Ashraf:** Software, Formal analysis. **Syed Saqib:** Validation, Supervision. **Touqeer Ahmad:** Methodology, Software. **Yasser Fouad:** Resources, Writing – review & editing, Funding acquisition. **Husnain Raza:** Formal analysis, Writing – original draft. **Umar Ashfaq:** Investigation, Writing – original draft. **Aamir Pervaiz:** Investigation, Resources.

Declaration of Competing Interest

The authors declare that they have no known competing financial interests or personal relationships that could have appeared to influence the work reported in this paper.

Data availability

No data was used for the research described in the article.

Acknowledgments

The authors extend their appreciation to the Researchers Supporting Project number (RSPD2023R698), King Saud University, Riyadh, Saudi Arabia for funding this research work.

The authors also acknowledge University College London for the technical support and APC by the transformative agreement.

References

[1] Kalghatgi G. Development of fuel/engine systems—the way forward to sustainable transport. Engineering 2019;5(3):510–8.
[2] Montanarella L, Vargas R. Global governance of soil resources as a necessary condition for sustainable development. Curr. Opin. Environ. Sustain. 2012;4(5):559–64.
[3] Leach F, et al. The scope for improving the efficiency and environmental impact of internal combustion engines. Transportat. Eng. 2020;1:100005.
[4] Simsek S, Ozdalyan B. Improvements to the composition of fusel oil and analysis of the effects of fusel oil–gasoline blends on a spark-ignited (SI) engine's performance and emissions. Energies 2018;11(3):625.
[5] Martins J, Brito F. Alternative fuels for internal combustion engines. Energies 2020;13(16):4086.
[6] Mathur S, Waswani H, Singh D, Ranjan R. Alternative Fuels for Agriculture Sustainability: Carbon Footprint and Economic Feasibility. AgriEngineering 2022;4(4):993–1015.
[7] Rony ZI, et al. Alternative fuels to reduce greenhouse gas emissions from marine transport and promote UN sustainable development goals. Fuel 2023;338:127220.
[8] Acheampong M, et al. In pursuit of Sustainable Development Goal (SDG) number 7: Will biofuels be reliable? Renew. Sustain. Energy Rev. 2017;75:927–37.
[9] Bhan C, Verma L, Singh J. In: Environmental Concerns and Sustainable Development: Volume 1: Air, Water and Energy Resources. Singapore: Springer Singapore; 2020. p. 317–31.
[10] Tsita KG, et al. Next generation biofuels derived from thermal and chemical conversion of the Greek transport sector. Therm. Sci. Eng. Progr. 2020;17:100387.

[11] Kalghatgi GT. Developments in internal combustion engines and implications for combustion science and future transport fuels. Proc. Combust. Inst. 2015;35(1):101–15.

[12] Aliramezani M, Koch CR, Shahbakhti M. Modeling, diagnostics, optimization, and control of internal combustion engines via modern machine learning techniques: A review and future directions. Prog. Energy Combust. Sci. 2022;88:100967.

[13] Kumar S, Kumar N, Vivekadhish S. Millennium Development Goals (MDGs) to Sustainable Development Goals (SDGs): Addressing Unfinished Agenda and Strengthening Sustainable Development and Partnership. Indian J. Community Med. 2016;41(1):1–4.

[14] Biermann F, Kanie N, Kim RE. Global governance by goal-setting: the novel approach of the UN Sustainable Development Goals. Curr. Opin. Environ. Sustain. 2017;26:26–31.

[15] Zhao W, et al. Technological and environmental advantages of a new engine combustion mode: Dual Biofuel Intelligent Charge Compression Ignition. Fuel 2022;326:125067.

[16] Costanza R, Daly L, Fioramonti L, Giovannini E, Kubiszewski I, Mortensen LF, et al. Modelling and measuring sustainable wellbeing in connection with the UN Sustainable Development Goals. Ecol. Econ. 2016;130:350–5.

[17] Shrivastava N, Khan ZM. Application of soft computing in the field of internal combustion engines: a review. Arch. Comput. Meth. Eng. 2018;25(3):707–26.

[18] Thodda G, Madhavan VR, Thangavelu L. Predictive modelling and optimization of performance and emissions of acetylene fuelled CI engine using ANN and RSM. Energy Sources Part A 2023;45(2):3544–62.

[19] Khandal SV, Razak A, Veza I, Afzal A, Alwetaishi M, Shaik S, et al. Hydrogen and dual fuel mode performing in engine with different combustion chamber shapes: Modelling and analysis using RSM-ANN technique. Int. J. Hydrogen Energy 2022.

[20] Sharma P, Chhillar A, Said Z, Memon S. Exploring the exhaust emission and efficiency of algal biodiesel powered compression ignition engine: Application of box–behnken and desirability based multi-objective response surface methodology. Energies 2021;14(18):5968.

[21] Veza I, Afzal A, Mujtaba MA, Tuan Hoang A, Balasubramanian D, Sekar M, et al. Review of artificial neural networks for gasoline, diesel and homogeneous charge compression ignition engine. Alex. Eng. J. 2022;61(11):8363–91.

[22] Yücesu HS, Sozen A, Topgül T, Arcaklioğlu E. Comparative study of mathematical and experimental analysis of spark ignition engine performance used ethanol–gasoline blend fuel. Appl. Therm. Eng. 2007;27(2-3):358–68.

[23] Simsek S, Uslu S. Investigation of the impacts of gasoline, biogas and LPG fuels on engine performance and exhaust emissions in different throttle positions on SI engine. Fuel 2020;279:118528.

[24] Najafi G, Ghobadian B, Tavakoli T, Buttsworth DR, Yusaf TF, Faizollahnejad M. Performance and exhaust emissions of a gasoline engine with ethanol blended gasoline fuels using artificial neural network. Appl. Energy 2009;86(5):630–9.

[25] Uslu S, Celik MB. Performance and exhaust emission prediction of a SI engine fueled with I-amyl alcohol-gasoline blends: an ANN coupled RSM based optimization. Fuel 2020;265:116922.

[26] Barboza AB, Mohan S, Dinesha P. On reducing the emissions of CO, HC, and NOx from gasoline blended with hydrogen peroxide and ethanol: Optimization study aided with ANN-PSO. Environ. Pollut. 2022;310:119866.

[27] T. Palani G.S. Esakkimuthu G. Dhamodaran A. Sundaraganesan Performance optimization of gasoline engine fueled with ethanol/n-butanol/gasoline blends using response surface methodology 1 13.

[28] Yusri IM, Mamat R, Azmi WH, Omar AI, Obed MA, Shaiful AIM. Application of response surface methodology in optimization of performance and exhaust emissions of secondary butyl alcohol-gasoline blends in SI engine. Energ. Conver. Manage. 2017;133:178–95.

[29] Kaliyaperumal, M., et al., Development of a fuzzy logic model for the prediction of spark-ignition engine performance and emission for gasoline–ethanol blends. Green Process. Synthes., 2023. **12**(1): p. 20230009.

[30] Yaman H, Yesilyurt MK, Uslu S. Simultaneous optimization of multiple engine parameters of a 1-heptanol/gasoline fuel blends operated a port-fuel injection spark-ignition engine using response surface methodology approach. Energy 2022;238:122019.

[31] Kapusuz M, Ozcan H, Yamin JA. Research of performance on a spark ignition engine fueled by alcohol–gasoline blends using artificial neural networks. Appl. Therm. Eng. 2015;91:525–34.

[32] Kumar AN, et al. Decanol proportional effect prediction model as additive in palm biodiesel using ANN and RSM technique for diesel engine. Energy 2020;213:119072.

[33] Khandal SV, Gadwal SB, Raikar VA, Yunus Khan TM, Badruddin IA. An experimental-based artificial neural network performance study of common rail direct injection engine run on plastic pyrolysis oil. Int. J. Sustain. Eng. 2021;14(2):137–46.

[34] Shivakumar, Srinivasa Pai P, Shrinivasa Rao BR. Artificial neural network based prediction of performance and emission characteristics of a variable compression ratio CI engine using WCO as a biodiesel at different injection timings. Appl. Energy 2011;88(7):2344–54.

[35] Liu, Z., et al., *An artificial neural network developed for predicting of performance and emissions of a spark ignition engine fueled with butanol–gasoline blends.* Adv Mechan Eng, 2018. **10**(1): p. 1687814017748438.

[36] Rezaei J, Shahbakhti M, Bahri B, Aziz AA. Performance prediction of HCCI engines with oxygenated fuels using artificial neural networks. Appl. Energy 2015;138:460–73.

[37] Shrestha, S., Z. Bochenek, and C. Smith. Artificial Neural Network (ANN) beyond cots remote sensing packages: Implementation of Extreme Learning Machine (ELM) in MATLAB. in 2012 IEEE International Geoscience and Remote Sensing Symposium. 2012. IEEE.

[38] Uslu S, Celik MB. Prediction of engine emissions and performance with artificial neural networks in a single cylinder diesel engine using diethyl ether. Eng Sci Technol Int J 2018;21(6):1194–201.

[39] Schrimpf, M., et al., *The neural architecture of language: Integrative modeling converges on predictive processing.* Proceed Natl Acad Sci, 2021. **118**(45): p. e2105646118.

[40] Deshwal D, Sangwan P, Kumar D. A language identification system using hybrid features and back-propagation neural network. Appl. Acoust. 2020;164:107289.

[41] Velmurugan A, Loganathan M, Gunasekaran EJ. Prediction of performance, combustion and emission characteristics of diesel-thermal cracked cashew nut shell liquid blends using artificial neural network. Front Energy 2016;10(1):114–24.

[42] Dhande DY, Choudhari CS, Gaikwad DP, Dahe KB. *Development of artificial neural network to predict the performance of spark ignition engine fuelled with waste pomegranate ethanol blends.* Informat Process Agricult 2022.

[43] Yap WK, Ho T, Karri V. Exhaust emissions control and engine parameters optimization using artificial neural network virtual sensors for a hydrogen-powered vehicle. Int J Hydrogen Energy 2012;37(10):8704–15.

[44] Deb M, Majumder P, Majumder A, Roy S, Banerjee R. Application of artificial intelligence (AI) in characterization of the performance–emission profile of a single cylinder CI engine operating with hydrogen in dual fuel mode: an ANN approach with fuzzy-logic based topology optimization. Int J Hydrogen Energy 2016;41(32):14330–50.

[45] Simsek S, et al. Improving the combustion process by determining the optimum percentage of liquefied petroleum gas (LPG) via response surface methodology (RSM) in a spark ignition (SI) engine running on gasoline-LPG blends. Fuel Process Technol 2021;221:106947.

[46] Simsek S, Uslu S. Determination of a diesel engine operating parameters powered with canola, safflower and waste vegetable oil based biodiesel combination using response surface methodology (RSM). Fuel 2020;270:117496.

[47] Abdalla AN, Tao H, Bagaber SA, Ali OM, Kamil M, Ma X, et al. Prediction of emissions and performance of a gasoline engine running with fusel oil–gasoline blends using response surface methodology. Fuel 2019;253:1–14.

[48] Yüksel F, Yüksel B. The use of ethanol–gasoline blend as a fuel in an SI engine. Renew Energy 2004;29(7):1181–91.

[49] Balki MK, Sayin C. The effect of compression ratio on the performance, emissions and combustion of an SI (spark ignition) engine fueled with pure ethanol, methanol and unleaded gasoline. Energy 2014;71:194–201.

[50] Iliev S. A comparison of ethanol and methanol blending with gasoline using a 1-D engine model. Procedia Eng 2015;100:1013–22.

[51] Celik MB, Özdalyan B, Alkan F. The use of pure methanol as fuel at high compression ratio in a single cylinder gasoline engine. Fuel 2011;90(4):1591–8.

[52] Najafi G, Ghobadian B, Yusaf T, Safieddin Ardebili SM, Mamat R. Optimization of performance and exhaust emission parameters of a SI (spark ignition) engine with gasoline–ethanol blended fuels using response surface methodology. Energy 2015;90:1815–29.

[53] Eyidogan M, Ozsezen AN, Canakci M, Turkcan A. Impact of alcohol–gasoline fuel blends on the performance and combustion characteristics of an SI engine. Fuel 2010;89(10):2713–20.

[54] Verma A, Dugala NS, Singh S. Experimental investigations on the performance of SI engine with Ethanol-Premium gasoline blends. Mater Today Proc 2022;48:1224–31.

[55] Koç M, Sekmen Y, Topgül T, Yücesu HS. The effects of ethanol–unleaded gasoline blends on engine performance and exhaust emissions in a spark-ignition engine. Renew Energy 2009;34(10):2101–6.

[56] Masum BM, Masjuki HH, Kalam MA, Rizwanul Fattah IM, Palash SM, Abedin MJ. Effect of ethanol–gasoline blend on NOx emission in SI engine. Renew Sustain Energy Rev 2013;24:209–22.

[57] Xie M, et al. Chemical kinetic investigation on NOx emission of SI engine fueled with gasoline-ethanol fuel blends. Sci Total Environ 2022;831:154870.

[58] Chansauria P, Mandloi R. Effects of ethanol blends on performance of spark ignition engine-a review. Mater Today Proc 2018;5(2):4066–77.

[59] Mohammed MK, et al. Effect of ethanol-gasoline blends on SI engine performance and emissions. Case Stud Therm Eng 2021;25:100891.

[60] Yücesu HS, Topgül T, Çinar C, Okur M. Effect of ethanol–gasoline blends on engine performance and exhaust emissions in different compression ratios. Appl Therm Eng 2006;26(17-18):2272–8.